Wave Source Localization Among Multiple Knife-Edges

Mikhail S. Lytaev(✉)

St. Petersburg Federal Research Center of the Russian Academy of Sciences, 14-th Linia, V.I., No. 39, Saint Petersburg 199178, Russia
mikelytaev@gmail.com

Abstract. The problem of localizing a monochromatic source in a two-dimensional unbounded environment is considered. The environment contains arbitrarily positioned thin vertical obstacles (knife-edges), leading to diffraction effects and multiple reflections. The problem is formulated using the method of adjoint equations. Two most commonly used types of the matched field processing (MFP) method are analyzed: Bartlett and minimum variance (MV). Numerical experiments are conducted for various arrangements of obstacles and receivers. It is shown that the MFP method can be successfully used for localizing radiation sources under conditions of multiple reflections.

Keywords: inverse problem · knife-edge diffraction · matched field processing · wave propagation · ill-posed problem · adjoint equation

1 Introduction

The search and localization of radiation sources based on measurement data belong to the class of inverse problems [5]. From a mathematical point of view, their complexity lies in their ill-posedness (in the sense of Hadamard) [8]. Commonly, it manifests in insufficient measurement data for the unambiguous determination of the source's location - there may be multiple possible solutions. The most obvious way to improve accuracy is by increasing the number and spatial coverage of measurements, although this comes with equally obvious practical difficulties. A significant reduction in uncertainty and hence an increase in localization accuracy can be achieved by incorporating information about the signal propagation environment. This approach requires knowledge of propagation environment in each specific case, as well as complex mathematical models that simultaneously account for arbitrary environmental inhomogeneities and measurements.

Significant progress in this field has been achieved in computational hydroacoustics. Since the late 1980s, the matched field processing (MFP) method has been actively developed [2]. Typically, the MFP method is applied in shallow and deep water waveguides, considering the sound speed height and range profiles as well as the profile and physical properties of the seabed. The method imposes

© The Author(s), under exclusive license to Springer Nature Switzerland AG 2024
O. Gervasi et al. (Eds.): ICCSA 2024, LNCS 14813, pp. 83–95, 2024.
https://doi.org/10.1007/978-3-031-64605-8_6

no restrictions on the relative placement of receivers, allowing it to be used for vertically and horizontally arranged arrays of hydrophones. There are extensions of this method for localizing multiple sources simultaneously [3,4]. The method can also be used for localizing moving sources [19]. Additionally, MFP has been successfully applied in seismology [14,18] and radar systems [7].

The aim of this study is to investigate the possibility of localization in conditions where diffraction and multiple reflections have a significant impact on the wave propagation. The study is based on a model environment with several vertically positioned thin impenetrable obstacles (so called knife-edges) [6,17]. This model is commonly used in radio physics to describe the radio wave propagation over complex terrain or in urban environments.

The paper is organized as follows. The next section presents the mathematical formulation of localizing a point source in a medium with multiple knife-edges. Section 3 proposes a general solution scheme based on the method of adjoint equations and demonstrates that the existing MFP-based localization methods are its consequence. Section 4 describes the solution scheme for the direct problem of computing the field from a known source, which is required for solving the inverse problem. Analysis of the results of numerical modeling is carried out in Sect. 5.

2 Problem Statement

The wave process is described by the two-dimensional Helmholtz equation, which we will write in operator form

$$A\psi = q,$$

where

$$A\psi = \frac{\partial^2 \psi}{\partial x^2} + \frac{\partial^2 \psi}{\partial z^2} + k^2 \left(1 + i\alpha\right) \psi,$$

α is a small parameter responsible for wave dissipation, k is the wavenumber, q is a point source of harmonic signals with an unknown amplitude Q at coordinates (x_s, z_s) that are need to be determined

$$q = Q\delta\left(x_s, z_s\right).$$

$\psi\left(x, z\right)$ is the spatial distribution of the complex field amplitude

$$\psi : \ \Omega \to \mathbb{C},$$

defined on half-plane

$$\Omega = \left\{(x, z) \,|x \in (-\infty, +\infty), z \in [0, +\infty)\right\}.$$

Dirichlet boundary condition is imposed at the lower boundary

$$\psi\left(x, 0\right) = 0, \ \ x \in (-\infty, +\infty).$$

There are M thin vertical impermeable obstacles, called "knife-edges". They are characterized by its distance x_i^e and height H_i^e. It is required that the Dirichlet boundary condition also be satisfied on the boundaries of the obstacles

$$\psi\left(x_i^e, z\right) = 0, \;\; z \in [0, H_i] \,.$$

A set of N measurements is given: $\{x_i^m, z_i^m, v_i\}$, where $i = 1 \ldots N$. Here, x_i, z_i are the coordinates of the measurements, and $v_i \in \mathbb{C}$ represents the complex amplitude.

The schematic representation of the problem setup is shown in Fig. 1.

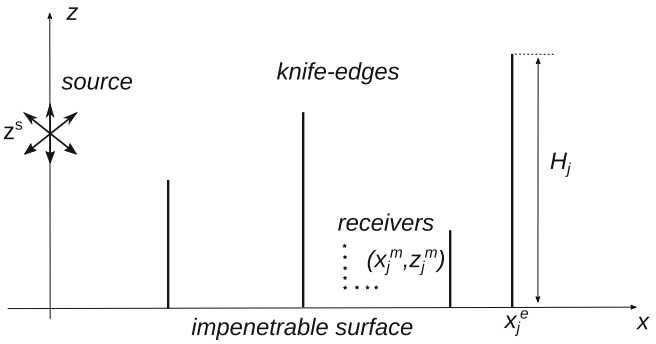


Fig. 1. Schematic description of the problem statement.

3 Matched Field Processing

For a mathematically rigorous derivation of the MFP method, we will utilize the method of adjoint equations [12], which is commonly employed in solving the inverse problems of various nature [13].

3.1 Adjoint Method Formulation

Consider a Hilbert space with a scalar product

$$(f, g) = \int_{\Omega} f \bar{g}$$

and adjoint operator [12] A^*, defined as follows

$$(Af, g) = (f, A^* g) \,. \tag{1}$$

Suppose we have a measuring device that records a certain integral characteristic of the field, i.e.

$$J_p(\psi) = \int\limits_{\Omega} \psi \bar{p} = (\psi, p).$$

In the simplest case, $p = \delta(x_m, z_m)$, which corresponds to measuring the field with a point receiver at some point (x_m, z_m).

Next we consider the following adjoint equation

$$A^* \varphi_p^* = p, \tag{2}$$

and substitute it into definition (1)

$$\left(A\psi, \varphi_p^*\right) = \left(\psi, A^* \varphi_p^*\right),$$

which gives us the following equalities

$$\left(q, \varphi_p^*\right) = (\psi, p) = J_p(\psi) = Q\bar{\varphi_p^*}(x^s, z^s). \tag{3}$$

By solving Eq. (3) with respect to (x_s, z_s), one can estimate the location of the original source. In particular, for a point receiver, this equation takes the following form

$$J_p(\psi) = \psi(x_i^m, z_i^m) = v_i = Q\bar{\varphi_p^*}(x^s, z^s).$$

Naturally, for a single receiver, such an equation does not have a unique solution. Additionally, the amplitude of the source Q is usually unknown. Therefore, for a more reliable determination of the source location, several spatially separated point receivers are required. Furthermore, in a real situation, measurements contain noise and uncertainties.

The main difference between the various MFP methods lies in the way of comparing and matching the value of the conjugate field and measurements. Next, we will consider the two most commonly used MFP methods: Bartlett and minimum variance (MV) [2].

3.2 Bartlett MFP Processor

We first describe the simplest and most widely used method. Consider the following vectors, made up of the measurements and their corresponding solutions of the adjoint Eqs. (2)

$$\mathbf{v} = \left(v_1\ v_2\ ...\ v_N\right)^T,$$

$$\mathbf{g}(x, z) = \left(\bar{\varphi^*}_{\delta(x_1, z_1)}(x, z)\ \bar{\varphi^*}_{\delta(x_2, z_2)}(x, z)\ ...\ \bar{\varphi^*}_{\delta(x_N, z_N)}(x, z)\right)^T.$$

The problem of localizing the source is formalized as the least squares minimization

$$\arg \min_{(x,z)\in\Omega} \min_{Q\in\mathbb{C}} ||\mathbf{v} - Q\mathbf{g}||^2. \tag{4}$$

The minimization problem with respect to Q can be easily solved analytically [11]. Then, the problem (4) can be rewritten as follows

$$\arg \max_{(x,z)\in\Omega} \frac{|\mathbf{v}^H \mathbf{g}(x,z)|^2}{||\mathbf{g}(x,z)||^2}. \tag{5}$$

In such a formulation, the maximization problem is solved by simple enumeration of all possible variants. The complexity of its solution is $O(n_x n_z N)$, where n_x and n_z are the sizes of the computational grid along x and z respectively. If necessary, various optimization methods or dimensionality reduction techniques can be employed to accelerate this procedure [11].

For convenience, we rewrite (5) as follows

$$\arg \max_{(x,z)\in\Omega} B_{Bart}(x,z),$$

where function $B_{Bart}(x,z)$ is called "processor" or "ambiguity surface" and is defined as follows

$$B_{Bart}(x,z) = |\mathbf{v}^H \mathbf{w}(x,z)|^2 = \mathbf{w}^H(x,z)\,\mathbf{K}\mathbf{w}(x,z),$$

where

$$\mathbf{w}(x,z) = \frac{\mathbf{g}(x,z)}{||\mathbf{g}(x,z)||},$$

$$\mathbf{K} = \mathbf{v}\mathbf{v}^H.$$

3.3 Minimum Variance

The main idea of this modification is to minimize the value of the ambiguity surface at all points in space except where the source is actually located [9]. The result is the following processor

$$B_{MV}(x,z) = \left[\mathbf{w}^H(x,z)\,\mathbf{K}^{-1}\mathbf{w}(x,z)\right]^{-1},$$

for which it is also necessary to find the maximum to determine the source location.

4 Multiple Knife-Edge Diffraction

As we saw in the previous section, the solution to the inverse problem is based on solving the direct one. That is, to determine the radiation source location based on field measurements, a method is required to compute the field value for an arbitrary source at an arbitrary point in space.

For simplicity and without loss of generality, we assume that the point source is located at the coordinates $(0, z_m)$. Then, following [17], the solution can be expressed as follows

$$\psi(x,z) = \sqrt{\frac{2}{\pi}} \int\limits_0^{+\infty} \tilde{\psi}(x,p) \sin(pz) dz,$$

where

$$\tilde{\psi}(x,p) = -\frac{k^2}{\sqrt{2\pi}} \sum_{j=1}^{M} \tilde{G}(x,x_j,p)\varphi_j(p) + \sqrt{\frac{2}{\pi}} \sin(z_m p)\, \tilde{G}(x,0,p), \tag{6}$$

$$\tilde{G}(x,x',p) = -\frac{1}{2\gamma(p)} e^{-\gamma(p)|x-x'|},$$

$$\gamma(p) = \sqrt{\frac{\sqrt{(p^2-k^2)^2+(k^2\alpha)^2} - (k^2-p^2)}{2}} - i\sqrt{\frac{\sqrt{(p^2-k^2)^2+(k^2\alpha)^2} + (k^2-p^2)}{2}}.$$

Functions $\varphi_j(p)$ satisfy the following system of integral equations

$$\begin{cases} \varphi_1(p) + \sum\limits_{j=1}^{M} \int\limits_{-\infty}^{+\infty} K_{1,j}(p,p')\varphi_j(p')dp' = g_1(p) \\ \varphi_2(p) + \sum\limits_{j=1}^{M} \int\limits_{-\infty}^{+\infty} K_{2,j}(p,p')\varphi_j(p')dp' = g_2(p) \\ \dots \\ \varphi_m(p) + \sum\limits_{j=1}^{M} \int\limits_{-\infty}^{+\infty} K_{m,j}(p,p')\varphi_j(p')dp' = g_m(p) \end{cases} \tag{7}$$

with kernel

$$K_{i.j}(p,p') \approx -\frac{bhk^2}{2\pi} \frac{\sin\left((p-p')\, H_i^e\right)}{(p-p')\,\gamma(p')} e^{-\gamma(p')|x_i^e - x_j^e|},$$

and right-hand side

$$g_i(p) \approx -bh\frac{2}{\pi} \int\limits_{-\infty}^{+\infty} \frac{\sin\left((p-p')\, H_i^e\right)}{2\,(p-p')\,\gamma(p')} \sin(z_m p')\, e^{-\gamma(p')x_i^e} dp'.$$

b and h are parameters responsible for the permeability and thickness of the obstacles, respectively. Furthermore, we assume that $bh = 400$, choosing this value ensures the required level of impermeability and allows us to consider the obstacle as negligibly thin. It should be noted that this model does not allow b and h to approach infinity and zero, respectively, just as in nature there are no infinitely impermeable or infinitely thin obstacles.

In work [17], it is justified that the numerical solution of system (7) is the most efficient for the given problem. In fact, the essentially two-dimensional problem is reduced to a one-dimensional one. A rigorous justification of the correctness of such an approach and the derivation of system (7) are presented in works [15,16].

The most closely related alternative is the two-way parabolic equation method [1]. It can account not only for knife-edges but also for other obstacles of arbitrary shape. However, there are issues with its theoretical justification and convergence speed [17]. Full-wave methods, such as the finite element method, require too much computational recourses even for very small integration domains. Ray methods cannot accurately account for diffraction and multiple reflections effects, which are significant in the considered problem.

5 Numerical Results and Discussion

This section presents the results of numerical modeling for various configurations of obstacles and receivers. The source in all examples is located at point $(0, 50)$ and emits a signal at a frequency of 300 MHz (1 m wavelength). The modeling process for each example consists of the following steps:

1. Compute the two-dimensional field distribution from the source ψ using the method from the previous section. It is depicted on the left figure in each example.
2. Choose N space points (x_i^m, z_i^m) corresponding to the receiver locations. The field value at these points is used as the measurement $\psi(x_i^m, z_i^m) = v_i$, forming the vector $\mathbf{v}$.
3. Compute N two-dimensional fields $\bar{\varphi}^*_{\delta(x_i,z_i)}(x, z)$ using the method from the previous section and form the vector-valued function $\mathbf{g}(x, z)$.
4. Use $\mathbf{g}(x, z)$ and $\mathbf{v}$ to compute the ambiguity surface using the two methods: Bartlett (B_{Bart}) and MV (B_{MV}). Their two-dimensional distributions are respectively shown on the central and right figures.
5. Find the point at which the ambiguity surface takes the maximum value. It will be the source location.

In all examples below, white asterisks denote the source position, and black asterisks denote the receiver positions.

The modeling was performed using the PyWaveProp software library developed by the author [10].

5.1 Free Space

First, we consider the obstacle-free space. A vertical array of receivers is located at a distance of 900 m from the source. There are 25 point receivers, uniformly distributed at heights of 10–60 m with a 2-m interval. The results of the simulation are shown in Fig. 2. The ambiguity surface obtained by the Bartlett method

provides a more "spread out" solution in space. However, the maximum coincides precisely with the location of the original source. The MV method provides a solution that practically eliminates uncertainty in determining the source, the maximum can only be seen with zoom. However, the determined maximum is 7 m away from the true position in distance and 0.4 m in height.

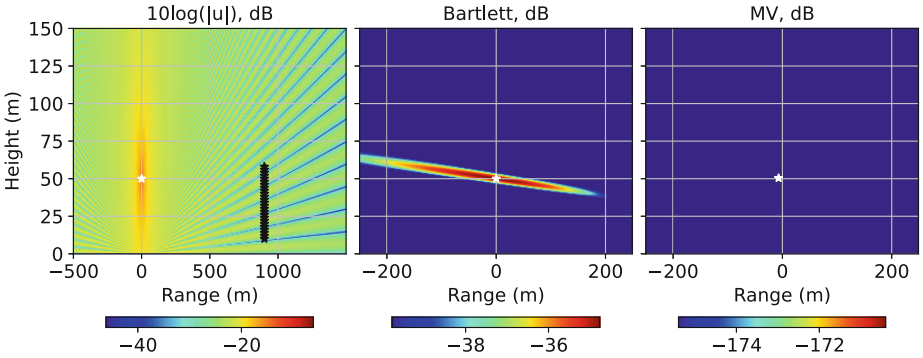


Fig. 2. Source localization in free space. Bartlett: (0, 50); MV: (-7, 50.4).

5.2 Source in Front of the Knife-Edge

Now we place a thin obstacle with a height of 70 m at a distance of 200 m behind the source. As seen in Fig. 3, the reflection from the obstacle did not hinder the determination of the source location. Moreover, the uncertainty in determining its location decreased for the Bartlett method. Both methods accurately determined the source location without errors. Apparently, it was facilitated by additional "information" contained in the reflected field.

5.3 Non Line of Sight

Now we move the obstacle in such a way that it ends up between the source and the array of receivers. So there is no direct line of sight between them. As seen in Fig. 4, the Bartlett method exhibits greater uncertainty in the area behind the obstacle. Nevertheless, it accurately determined the location of the source. However, the MV method, despite the absence of uncertainty, incorrectly detected the source location.

5.4 Two Knife-Edges

Next example is a scenario where the source and the receiver are located between two obstacles. Besides diffraction, the effects of multiple reflections between obstacles are significantly pronounced in this example. As seen in Fig. 5, even in these complex conditions, both methods generally correctly determine the position of the source.

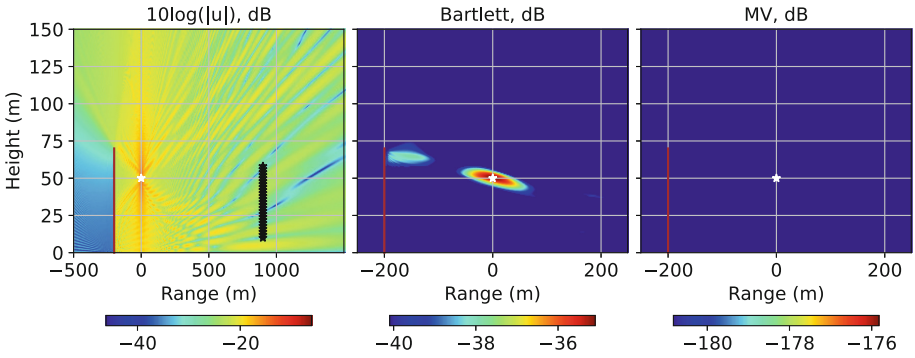


Fig. 3. Source localization in a presence of single knife-edge. Bartlett: (0, 50); MV: (0, 50).

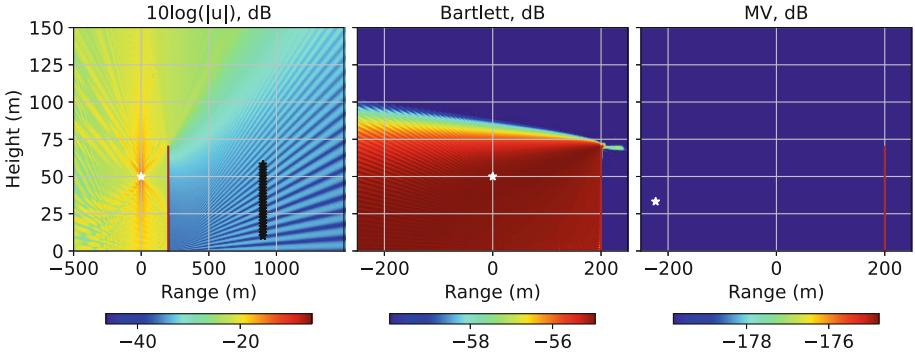


Fig. 4. Source localization in the absence of line of sight. Bartlett: (0, 50); MV: (−223, 33.2).

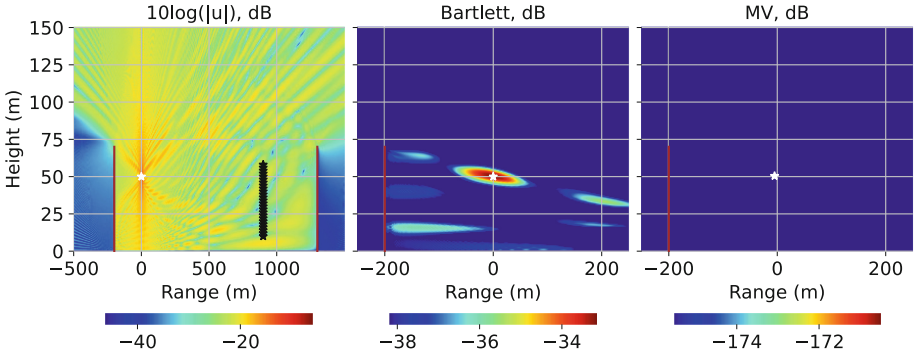


Fig. 5. Source localization between two knife-edges. Bartlett: (0, 50); MV: (−5, 50.4).

5.5 Horizontal Arrangement of Receivers

Next, we arrange the array of sources horizontally. 20 point receivers are positioned at distances ranging from 500 to 1000 m from the source at a height of 10 m. The results are shown in Fig. 6. The Bartlett method exhibits slightly greater uncertainty compared to the previous example. However, the position was detected correctly by both MFP processors.

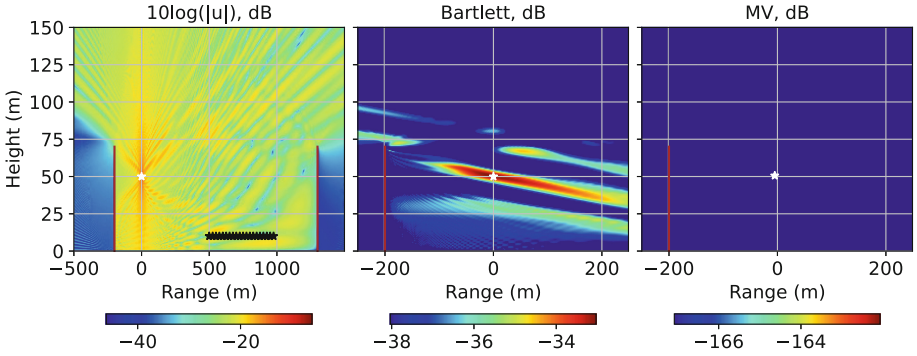


Fig. 6. Source localization using a horizontal array of receivers. Bartlett: (0, 50); MV: (−5, 50.6).

5.6 Multiple Knife-Edges

To demonstrate the capabilities of the method under consideration, we examine an environment with four obstacles. It is evident that the complexity of system (7) increases with the number of obstacles M. Nevertheless, the method easily allows for the consideration of 5–7 obstacles on a standard personal computer. If the size of the system exceeds the computer's memory capacity, its solving becomes practically impossible. The same problem arises within the finite element method, but for a significantly smaller number of obstacles and computational domain.

The results are shown in Fig. 7. As we can see, increasing the number of obstacles increases the uncertainty of the Bartlett method. However, the position was detected correctly. On the other hand, the error of the MV method amounted to 23 m in distance.

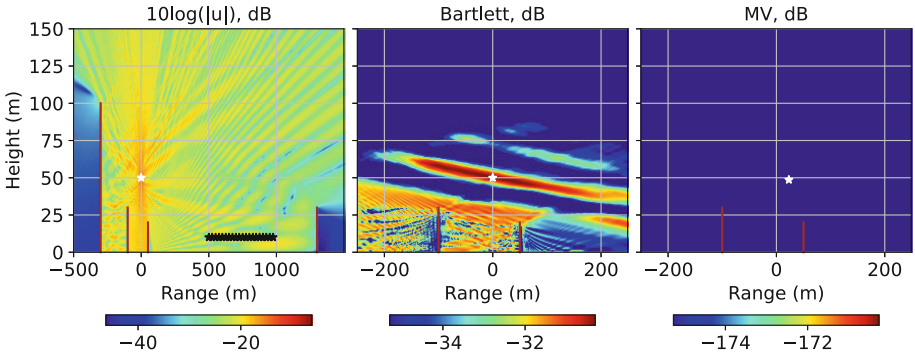


Fig. 7. Source localization among multiple obstacles. Bartlett: (0, 50); MV: (23, 48.6).

Summary results for all six examples are shown in Table 1. It is evident that the Bartlett method perfectly determined the source position in all cases. However, the MV method almost always yielded results with some degree of error.

Table 1. Summary table of the localization results.

Example	Number of obstacles	Line of sight	Bartlett	MV
1	0	yes	(0, 50)	(−7, 50.4)
2	1	yes	(0, 50)	(0, 50)
3	1	no	(0, 50)	(−223, 33.2)
4	2	yes	(0, 50)	(−5, 50.4)
5	2	yes	(0, 50)	(−5, 50.6)
6	4	yes	(0, 50)	(23, 48.6)

6 Conclusion

It is impossible to encompass all the variety of possible scenarios and configurations in one paper, but the software library PyWaveProp developed by the author [10] enables researchers to conduct computational experiments similar to those outlined above.

The main achievement of this work lies in demonstrating the capability of precise source localization simultaneously in conditions of interference, diffraction, and multiple reflections. These effects are encountered in signal propagation in densely built urban areas or complex underwater conditions. The most widely used Bartlett method demonstrated excellent results. The MV method obviously needs some improvements to be used in the multiple reflections scenarios.

This study focused only on a basic model scenario. The problem considered in this study for a monochromatic source can be easily generalized to the case of broadband sources. Further plans include addressing a more realistic scenario considering noise and other uncertainties in the environment. Additionally, the two-way parabolic equation is intended to be used for source detection among vertical inhomogeneities of arbitrary shape.

Acknowledgments. This study was supported by the Russian Science Foundation grant No. 23-71-01069.

References

1. Apaydin, G., Ozgun, O., Kuzuoglu, M., Sevgi, L.: A novel two-way finite-element parabolic equation groundwave propagation tool: tests with canonical structures and calibration. IEEE Trans. Geosci. Remote Sens. **49**(8), 2887–2899 (2011)
2. Baggeroer, A.B., Kuperman, W.A., Mikhalevsky, P.N.: An overview of matched field methods in ocean acoustics. IEEE J. Oceanic Eng. **18**(4), 401–424 (1993)
3. Collins, M.D., Fialkowski, L.T., Kuperman, W., Perkins, J.S.: The multivalued Bartlett processor and source tracking. J. Acoust. Soc. Am. **97**(1), 235–241 (1995)
4. Collins, M.D., Fialkowski, L.T., Lingevitch, J.F.: Localizing submerged acoustic sources under adverse conditions. J. Theor. Comput. Acoust. **30**(01), 2230001 (2022)
5. Colton, D., Kress, R.: Inverse Acoustic and Electromagnetic Scattering Theory. Springer, Cham (2012)
6. Deygout, J.: Multiple knife-edge diffraction of microwaves. IEEE Trans. Antennas Propag. **14**(4), 480–489 (1966)
7. Gingras, D.F., Gerstoft, P., Gerr, N.L., Mecklenbrauker, C.: Electromagnetic matched field processing for source localization. In: 1997 IEEE International Conference on Acoustics, Speech, and Signal Processing, vol. 1, pp. 479–482. IEEE (1997)
8. Goncharsky, A., Stepanov, V., Tikhonov, A., Yagola, A.: Numerical Methods for the Solution of ill-Posed Problems. Springer, Dordrecht (1995). https://doi.org/10.1007/978-94-015-8480-7
9. Jensen, F.B., Kuperman, W.A., Porter, M.B., Schmidt, H.: Computational Ocean Acoustics. Springer, Cham (2014)
10. Lytaev, M.S.: PyWaveProp (2024). https://github.com/mikelytaev/wave-propagation
11. Mantzel, W., Romberg, J., Sabra, K.: Compressive matched-field processing. J. Acoust. Soc. Am. **132**(1), 90–102 (2012)
12. Marchuk, G.I.: Adjoint Equations and Analysis of Complex Systems, vol. 295. Springer, Cham (2013)
13. Marchuk, G.I.: Mathematical Models in Environmental Problems. Elsevier (2011)
14. Schippkus, S., Hadziioannou, C.: Matched field processing accounting for complex earth structure: method and review. Geophys. J. Int. **231**(2), 1268–1282 (2022)
15. Vavilov, S.A., Lytaev, M.S.: Modelling equation of electromagnetic scattering on thin dielectric structures. J. Math. Sci. **238**(5), 621–670 (2019)
16. Vavilov, S., Lytaev, M.: Electromagnetic waves scattering on an array composed of thin dielectric objects. J. Math. Sci. **243**, 689–697 (2019)

17. Vavilov, S.A., Lytaev, M.S.: Modeling equation for multiple knife-edge diffraction. IEEE Trans. Antennas Propag. **68**(5), 3869–3877 (2020)
18. Walter, F., et al.: Distributed acoustic sensing of microseismic sources and wave propagation in glaciated terrain. Nat. Commun. **11**(1), 2436 (2020)
19. Zala, C.A., Ozard, J.M.: Matched-field processing for a moving source. J. Acoust. Soc. Am. **92**(1), 403–417 (1992)